www.elsevier.com/locate/fuproc

Alkali/Chloride release during refuse incineration on a grate: Full-scale experimental findings

Martin Bøjer[a], *Peter Arendt Jensen*[a,*], *Flemming Frandsen*[a], *Kim Dam-Johansen*[a], *Ole Hedegaard Madsen*[b], *Kasper Lundtorp*[b]

[a]*CHEC Research Centre, Department of Chemical Engineering, Technical University of Denmark, Building 229, DK-2800 Lyngby, Denmark*
[b]*Babcock & Wilcox Vølund ApS, Odinsvej 19, DK-2600 Glostrup, Denmark*

ARTICLE INFO

Article history:
Received 11 December 2006
Received in revised form
12 October 2007
Accepted 16 October 2007

Keywords:
Waste
Incineration
Alkali
Chlorine
Volatilisation
Grate
Boiler
Corrosion

ABSTRACT

Waste to energy (WtE) plants are utilised for the production of heat and electricity. However, due to corrosion at super heater surfaces a relatively low 25% of the waste lower heating value can with the present technology be converted to electricity. High contents of Cl, Na, K, Zn, Pb and S in waste cause relatively high super heater corrosion rates. The Cl-content in waste is one of the key-factors for volatilisation of alkali and heavy metals in WtE plants. Little is known about the release of Cl, Na, K, Zn, Pb, and S along grate of waste incineration plants. The 26 t h^{-1} WtE plant Vestforbrænding unit 5 in Denmark was used for measurements of temperature, gas-concentration (O_2/CO/CO_2), and sampling of gas phase Cl, Na, K, Pb, Zn, and S. Unit 5 has 6 ports distributed along the 13 m long grate between 1.5–1.8 m above the grate. Five of these ports were used for measurements. Two aqueous absorption systems containing a solution of NH_3 or a solution of H_2O_2/HNO_3 were used to collect the gaseous samples. Tar was found to condense in the sampling system at the ports near the fuel inlet. The experiments showed the majority of Cl, Na, and K to be volatilised during the early stages of combustion. The maximum release of Cl, Na, and K was measured in port 2 as 177 ppm_v, 71 ppm_v, and 44 ppm_v respectively. The maximum average gas temperature of 1140 was measured in port 3 compared to the temperatures at ports 2 and 4 of 816 and 551 respectively. It has been suggested to use flue gas from the area of the grate near port 3 with a high temperature, that contains relatively low amounts of corrosive elements, and lead to a separate high temperature super heater and thus increase the electrical efficiency.

1. Introduction

Boiler corrosion constitutes a significant problem in electricity-producing waste-to-energy (WtE) plants, causing loss of material, frequent shut-downs for maintenance, and high operational cost. Deposits with a high Cl content, in particular, induce a high corrosion rate on super heater tubes.

The release of the volatile elements Cl, Na, K, Pb, Zn, and S to the flue gas and the aerosol formation from those volatile elements is of special interest. The volatile elements are present in deposit layers at high concentrations where they may form low-temperature slags able to induce high corrosion rates. The release of elements is a result of volatilisation but can to some degree be caused by particle entrainment. Measurement of the concentration and the location of the release of Cl, Na, K, Pb, Zn, and S from the grate, combined with information on the magnitude and location of the heat flux from the grate, may be used to isolate the region of the flue gas that has a high heat flux, but low concentrations of corrosive elements. This isolated portion of the flue gas may

* *Corresponding author*. Tel.: +45 4525 2849; fax: +45 4588 2258.
E-mail address: paj@kt.dtu.dk (P.A. Jensen).

0378-3820/$ – see front matter © 2007 Elsevier B.V. All rights reserved.
doi:10.1016/j.fuproc.2007.10.003

be directed to a separate super heater section, where it can raise the steam temperature. The elevated super heater steam temperature could then increase the electrical efficiency of the WtE plant.

1.1. *Volatilisation*

The volatilisation of elements to the flue gas depends on the fuel composition [1], the local oxidative/reducing environment, the primary air, and the temperature [2]. The fuel composition varies over time, with seasons, and with region [3].

The release of ash-forming elements from the grate combustion zone during incineration has been studied primarily by examining the overall mass balance of a plant [4]. The fractions of different elements remaining in the bottom ash for a waste of residential origin (household waste) and a mixed waste of residential and commercial origins are given in Table 1. The data originates from a full-scale grate-type waste incineration plant with a capacity of 5.2 t of waste per hour, and an average furnace room-temperature of 820–880 °C [4]. The two waste feed compositions differ mostly within the uncertainty of the analyses. The split between bottom ash and flue gas for the species does not differ significantly for the two investigated feeds. About 90% of the chlorine is released and about half of Pb and Zn is released. Approximately 10% of Na and 33% of K is released. More than 75% of S is released. The elements Ca, Al, Fe, and Si are less volatile (>88% of these elements remains in the bottom ash) and account for approximately 10% of the feed and they are the main components of the ash fractions [4].

The chlorine content in the feed has proven to be critical for corrosion on super heater surfaces [6,7]. The chlorine content is significantly higher in municipal solid waste (MSW) (~0.7 wt.% [5], 0.45–0.72 wt.% [8]), compared to coal (maximum levels ~0.25 wt.% [9]). The release of Pb, Zn, Na, and K is strongly influenced by the content of chlorine in the fuel. A lab-scale experiment was conducted by Chang et al. by adding $CaCl_2$ and Cl_2 to fly-ash and then studying the effect on volatilisation at 1000 °C for 3 h [10]. As seen in Table 2, a significant increase in the volatilisation of the elemental species K, Na, Pb, and Zn was observed, compared to measurements without chlorine addition [11].

Table 1 – Content of selected elements in the feed and fraction of the elements that remains in the bottom ash of the feed input [5]

	Household waste		Mixed waste	
Component	Feed composition [wt.%]	Fraction in bottom ash [%]	Feed Composition [wt.%]	Fraction in bottom ash [%]
H_2O	29±4	–	24±3	–
Cl	0.73±0.12	9±2	0.69±0.11	10±2
K	0.25±0.05	67±5	0.23±0.04	67±5
Na	0.48±0.12	89±3	0.51±0.12	92±2
S	0.14±0.02	24±5	0.13±0.02	19±4
Pb	0.053±0.011	59±7	0.070±0.013	44±7
Zn	0.13±0.03	53±9	0.16±0.03	43±8
Cu	0.082±0.033	97±1	0.078±0.031	96±1
Ca	2.4±0.6	89±3	2.4±0.6	92±2
Al	1.3±0.3	88±2	1.1±0.3	91±2
Fe	3.1±0.8	99.2±0.2	2.7±0.7	98.9±0.3
Si	3.8±0.9	95±1	3.7±0.8	97±1

Table 2 – Effect of $CaCl_2$ and Cl_2 addition on volatilisation from fly ash sample at 1000 °C for 3 h

Element	Volatilisation w/o Cl-addition [11] [wt.%]	Volatilisation w. Cl-addition [10] [wt.%]
Pb	90	94.8–96.1
Zn	40	96.5–100
Na	62	75.3–75.5
Ks	76	90.1–93.0

Equilibrium results from thermodynaic equilibrium calculations may be used to indicate the volatilisation of species from the grate of a waste incinerator though unlikely able to completely predict the actual behaviour in a large, heterogenous, and time-limited system. Sørum et al. [12] found by use of thermodynamic equilibrium calculations, that increasing the original content of chlorine in the fuel (0.56 wt.%) 10 times would probably lower the temperature at which Cu, Ni, and Zn are fully volatilised from 970, 1520, and 1670 to 670, 1000, and 780 K respectively. Watanabe [13] investigated the release of chlorine from a synthetic waste in the temperature range 500–900 °C. The released fraction was captured in an absorbing liquid. As seen in Fig. 1, about half of the chlorine was volatilised and then recovered in the absorber at a temperature of 500 °C. The non-volatilised chlorine remained in the residue. Volatilisation of chlorine increased with temperature until nearly full volatilisation was achieved at 900 °C. Compared to the measured 70-100% release of chlorine from wood at 500 °C [14] the 50% released at 500 °C seems relatively low. The 90% release of chlorine at 900 °C confirms the full-scale findings shown in Table 1 with 10% remaining in the bottom ash. Concentrations measurements of Na, K, Pb, Cd, Cu, and Sn prior to the flue gas cleaning system have been performed using ICP–OES [15]. Measurements of the flue gas concentration after the outlet of a rotary kiln of a hazardous waste incinerator have been performed at 1200 °C for Zn and Pb using ICP–OES [16]. The release profile of O_2, CO, CO_2, CH_4,

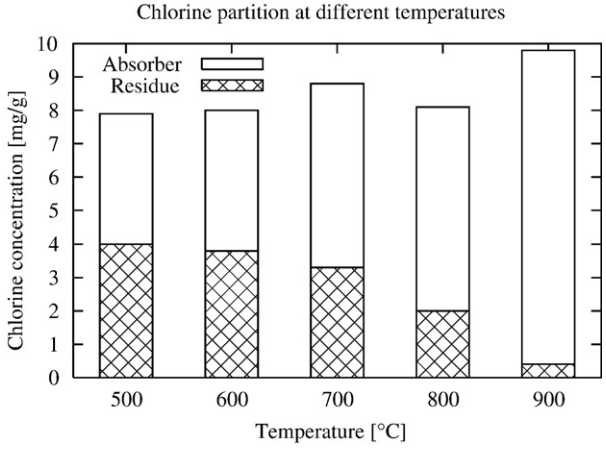

Fig. 1 – Chlorine partition between the residue (non-volatilised part) and the absorber (volatilised part) [mg g^{-1}].

H_2, H_2O, and organic carbon along the grate of the pilot waste incinerator, TAMARA, was investigated by Frey et al. [17].

No data however have been reported in the literature on the local release profile along and above a full-scale grate of the elements: Cl, Na, K, Zn, Pb, and S. Research on the release of the radioactive heavy metal isotopes of Zn and Cu, along a lab-scale, forward-acting grate with 3 zones has been conducted [18]. A known amount of the isotopes were added to a synthetic municipal waste that was being fed at a rate of 60 kg h^{-1} and having an average fuel residence time on the grate of 1 h After 20 min 80% of the Zn-isotopes were volatilised, with the greatest release taking place in the first zone. At the end of the third zone, the Zn-isotopes were fully volatilised. The Cu-isotopes gradually volatilised reaching a maximum of 5% volatilisation of the total amount of Cu-isotopes. It is s therefore concluded that Zn is significantly more volatile than the Cu. The measurements also suggested Zn to be released early in the combustion phase within the end of the 2nd zone, though no data regarding the zone of visible flames were available in the article.

1.2. *Deposits and corrosion on the super heater surfaces*

Chemical attack caused by deposits formed on super heaters and water tube walls is considered to be the primary cause of corrosion in waste incineration plants [19]. The deposits are formed by species, either condensing on the surface, or attaching as fly ash particles from the flue gas [20]. The ash deposit may form low-melting chlorides of alkali metals and heavy metals, of which many mixtures have melting points below 500 °C [19] (see Table 3). Chlorides of the alkali metals, sodium (Na) and potassium (K), and the heavy metals, zinc (Zn) and lead (Pb), are the species believed to be the most chemically aggressive and the ones primarily responsible for corrosion. A high corrosion rate occurs especially when the deposit is melted [19,22].

Typical concentration ranges of some elements in deposits from waste incineration plants are given in Table 4. The elements Cl, Na, K, Pb, Zn, and S are volatile and greatly influence the corrosive properties of the deposit on the super heater surface.

Nakagawa [7] investigated the corrosion rate of two alloys, a carbon steel and type 347 H steel, under various gas compositions, deposit compositions, and temperatures (300–400 °C) exposed over a period of 50 h. It was concluded that in order to have a high corrosion rate, a deposit must be present. A NaCl/KCl deposit on the metal in a HCl-rich gas (0.2 vol.%) induces a large weight loss of approximately 62 mg/cm^2 carbon steel at 350 °C, though a weight loss of only 1–2 mg/cm^2 was observed at 300 °C. The addition of CuO and ZnO to the deposit dramatically increased the corrosion effects on 347 H, though the addition of PbO did not cause any effects at the temperatures used in the experiments. Zn and Pb were therefore deemed to be the heavy metals of greatest interest in this investigation. Corrosion of super heater surfaces thus also depends on the extent of trace/heavy metal (Pb, Zn, and Cu) release from the fuel.

Table 3 – Eutectic compositions with low melting points

Eutectic Mixture [mole %]	Melting point [°C]	Reference
25 NaCl–75 $FeCl_3$	156	[6]
37 $PbCl_2$–63 $FeCl_3$	175	[6]
70 $ZnCl_2$–30 $FeCl_3$	200	[6]
55 $ZnCl_2$–45 KCl	230	[6]
70 $ZnCl_2$–30 NaCl	262	[6]
29$ZnCl_2$-67KCl-4$PbCl_2$	275	[21]
$ZnCl_2$	318	[21]
28NaCl-56KCl-16$PbCl_2$	400	[21]
70 $PbCl_2$–30 NaCl	410	[6]
52 $PbCl_2$–48 KCl	411	[6]
80 $PbCl_2$–20 $CaCl_2$	475	[6]
$PbCl_2$	498	[21]
49 NaCl–51 $CaCl_2$	500	[6]

Table 4 – Elemental concentrations [wt.%] of super heater deposits in waste incineration plants and a straw fired plant

Cl	S	Na	K	Pb	Zn	Reference
2–7	4–9	2–7	2–12	26–68	7–15	[20]
0.6	14.01	0.79	–	3.76	3.32	[23]
0.5	–	–	–	7.4	2.3	[21, Deposit 1]
0.1	–	–	–	1.6	2.9	[21, Deposit 2]
1.2	–	–	–	7.5	9.7	[21, Deposit 3]
23.7	10.2	–	33.8	–	–	[24, Strawfired plant]

1.3. *Electrical efficiency*

The electrical efficiency of a modern grate-fired WtE plant was reported to be ~25% (420 °C steam) [25] compared to a modern coal-fired plant at ~47% (580 °C steam) [26].

In a waste incineration plant the corrosion-rate is reported to increase exponentially for carbon steel at metal temperatures above 427 °C (800 F) and at constant flue gas temperature at 843 °C (1550 F) [6]. The corrosion-rate increases linearly with increasing metal-temperature at a constant flue-gas temperature of 760 °C (1400 F). With coal-firing Henderson et al. [27] found allowable super heater surface metal temperature up to 680 °C for select super heater metals.

In order to reduce this high temperature corrosion effect, an evaporator tube wall reduces the flue gas temperature to ~650 °C before entering the super heater sections [28]. Also a relatively lower steam temperature and pressure in the super heaters reduce the metal temperature and hence the corrosion rate, but they also reduce the electrical efficiency of a given plant.

1.4. *Objective*

The species Cl, Na, K, Zn, Pb, and S are present in the super heater deposit layers and promote corrosion on these metal surfaces at relatively low temperatures, by forming corrosive melts. Cl has been seen to promote volatilisation of alkali and heavy metals and to lower the melting temperature of ashes. It is the objective of the present study to measure a concentration profile of the elements Cl, Na, K, Zn, Pb, and S as function of location on the grate in a waste to energy boiler.

A heat flux and chlorine release profile along the grate will provide information on where the heat is released with the

Table 5 – Vestforbrænding, Unit 5 specifications

Nominal capacity	26 t h^{-1}
Nominal energy production [a]	66 MW
Nominal electricity production	16 MW
Steam pressure	55 bar
Steam temperature	380 °C
Primary air flow	up to 154,700 $Nm^3 h^{-1}$ at 60 °C
Secondary air flow	up to 46,400 $Nm^3 h^{-1}$
Recirculated flue gas [b]	up to ~112,000 $Nm^3 h^{-1}$ at 180 °C

[a] At lower heating value (LHV) 12 MJ kg^{-1}.
[b] Up to 27% of clean flue gases after electrostatic precipitor.

lowest concentrations of corrosion promoting species in the flue gas.

This will test the possibility for partitioning the flue from the grate and into two or more fractions having one fraction of the flue gas with a high heat flux and a low chlorine concentration. That fraction could be used in a high temperature super heater to increase the electricity efficiency of WtE plants. The flue gas fractions should then be united after use to dilute the fraction with a high chlorine concentration. Additionally the measured data combined with a temperature profile and the local gas concentrations of CO, CO_2, and O_2 will supply more realistic boundary conditions for CFD-modelling.

It is the primary objective of this paper to provide information on the local gas temperature, and the release of the corrosion-promoting elements Cl, Na, K, Zn, Pb, and S at different positions along the grate, in a full-scale WtE plant. It is also desired, as a secondary objective, to gain experience on performing measurements close to the grate surface of a full-scale waste incineration plant.

2. Experimental

All measurements were conducted at Vestforbrænding Unit 5 — a heat and power generating WtE plant in Glostrup, Denmark. Table 5 shows specifications for the plant that was

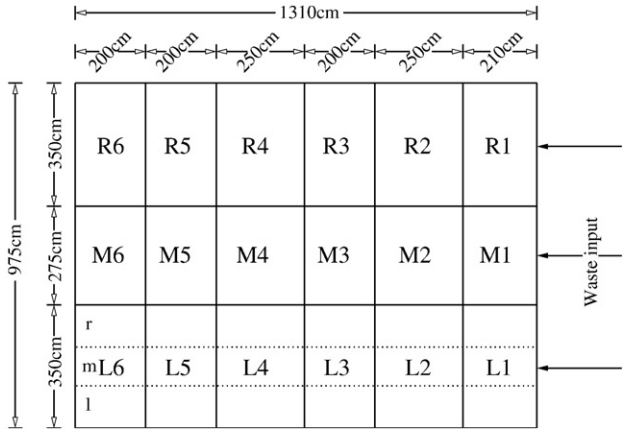

Fig. 2 – Sketch of the grate zones viewed from above and the respective dimensions. L, M and R prefixes denominates left, middle and right zones respectively. L_r, L_m, and L_l denominates a subdivision of the left zone for estimating the coverage visible flames.

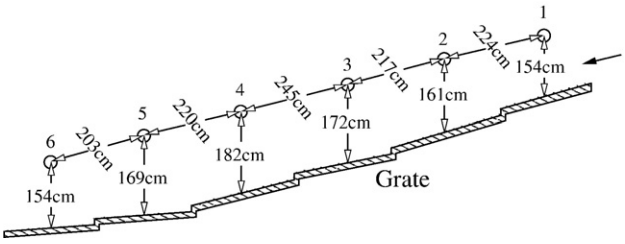

Fig. 3 – Sketch of the location of ports 1–6 relative to other ports and relative to the grate. The black arrow indicates the waste input direction.

commissioned in 1998. The refuse is incinerated on a hydraulically operated forward-acting grate which is 9.75 m wide and 13.1 m long, and consists of 18 zones. Each zone is supplied with individually controlled primary air (see dimensions in Fig. 2).

The refuse came from Copenhagen households and companies. The waste was mixed by three automatic operated cranes. No further sorting or treatment of the waste was done.

The location of the measuring positions (1–6) relative to the grate is shown in Fig. 3. The measurements were performed by inserting the probe into the designated ports L2, L3, L4, L5, and L6 placing the end of the probe above the center of each left grate section. It was not possible to measure at port L1 due to the waste being above, or level with the port during the time of the experiments. The depth of the inserted probe, as seen from the end of the grate, is shown in Fig. 4.

2.1. *Data collection and sampling methods*

During the experiments the Unit 5 boiler was running stably and did not experience malfunctions. Data collected from the plant control system showed the electrical energy production was 14.4 MW ± 0.8 MW. The steam pressure was 54.6 bar ± 0.6 bar, and the steam production was 102.4 t h^{-1} ± 5.1 t h^{-1}, which are at normal levels for the boiler unit.

Primary, secondary, and recirculation airflow measurements were obtained from the plant surveillance and control system.

A VHS video recording was made of the grate by using the plant's internal video surveillance system. The view of where the flames were on the grate was used in the control room as a

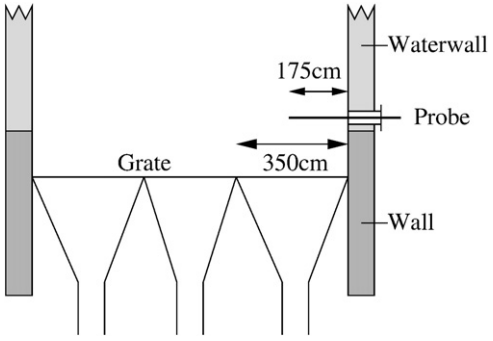

Fig. 4 – Sketch of the probe penetration into the freeboard through a port on the side of the incineration chamber.

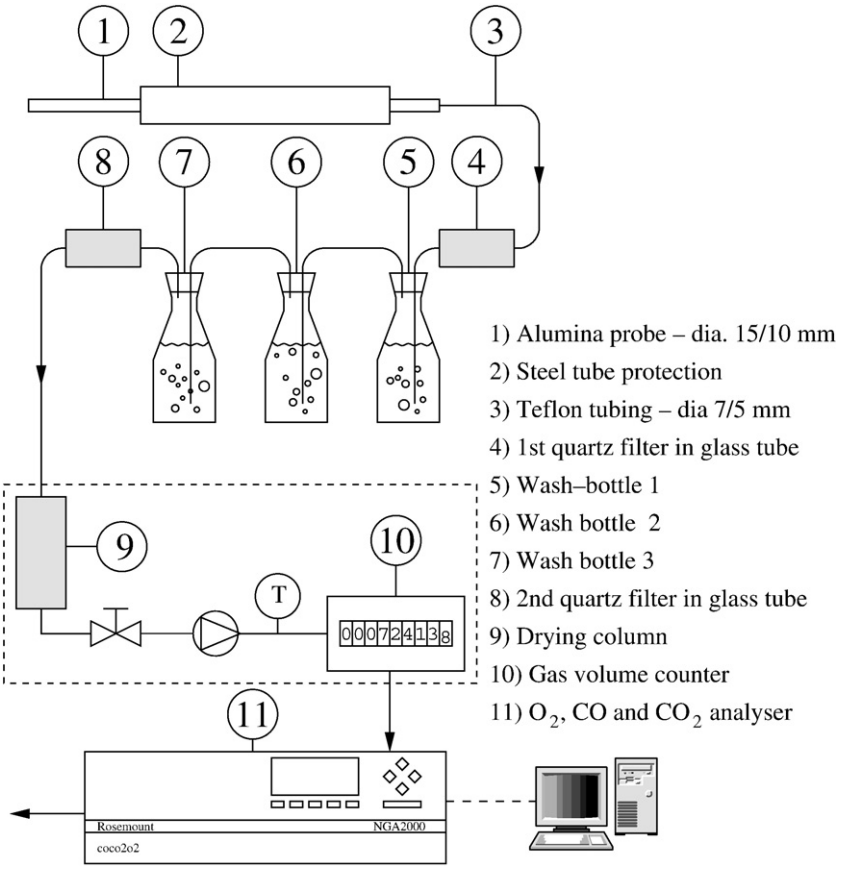

Fig. 5 – General flue gas sampling setup with the three wash bottles as the core of the system.

reference for controlling the combustion process. Here it will help to define where visible combustion flames appeared on the grate.

The local gas temperature above the grate was measured using a suction pyrometer (IFRF-model [29]). The suction pyrometer provides the actual gas temperature of the flue gas by avoiding the contribution of radiation to the temperature measurements. Wet sampling of the flue gas was performed to measure the local concentration of Cl, Na, K, Zn, Pb, and S using the sampling system described in Fig. 5. The same sampling system was also used as a filter front end for an optional gas concentration analysis of O_2, CO and CO_2. The 2.1 m straight fragile alumina probe (1) may either be inserted directly into one of the ports or through an optional protective steel tube (2). The Teflon tube (3) is attached to the alumina probe using Teflon tape to make the connection airtight. The Teflon tube is attached to the glass-tube (4) which contains pure quartz-filter material. The glass-tube connects to a series of three wash-bottles (5–7) in which the flue gas from the incinerator is bubbled through the liquid. Wash-bottle 3 (7) connects to a glass tube (8) containing pure quartz wool used for filtering particles. Each of the glass-connections (4–8) is airtight using grease and clamps. The second glass-tube containing pure quartz wool (8) is connected to a water drying and pumping system (9–10) via a Teflon-tube with airtight connections (ensured with Teflon-tape). Water is absorbed in the drying column (9), and the amount of dry gas is determined in the gas volume counter (10). Optionally a gas analyser (11) can be attached to the system using a Teflon-tube and Teflon-tape. The solutions A and B, shown in Table 6, are used in the wash-bottles for capturing different types of elements.

The alumina probe with an inner diameter of 10 mm was inserted at a 90° angle to the flue gas. No pitot tube was used to estimate the velocity of the flue gas above the grate. At the sampling rate of 2 NL/min the flue gas velocity was estimated to be approximately 30–40% lower than the velocity inside the tip of the alumina probe.

The first use of the sampling system in port L2 resulted in a the pressure system drop from −0.2 bar gauge to −0.8 bar gauge within 1 h, which indicated the system was clogged. The Teflon tube after the alumina probe was completely black with tar, and the second quartz filter was also black with tar. At this point extra quartz-filter material was added to the first filter and the experiment was rerun. When the pressure drop increased it was sufficient to exchange the Teflon tube and continue the experiment until the next pressure drop occurred and the sampling was stopped. The amount of tar in the Teflon tube and

Table 6 – Wash bottle solutions

Solution	Elements	Standard
A: 0.75% NH_3	Cl, Na, K and Ca	DS/EN 1911 using NH_3 instead of NaOH
B: 4.5% HNO_3 and 1.7% H_2O_2	Pb, Zn and S capture by oxidation	EN 14385 and ISO 11632

in the filters was less at port L3 than at port L2, and at port L4 it was less dark and more gray. At port L5 and L6 no tar was found in the sampling system. Due to the tar condensation and the amount of alumina probes available, it was not possible to reproduce the experiments and hence only one gas sampling experiment was performed for Cl, Na, and K at the ports L2–L6, and only one gas sampling experiment for Pb, Zn, and S at the ports L5–L6. The alumina tubes, the Teflon tubes and the filters with tar were stored in plastic containers for later analysis.

A possible solution to addressing the tar could be to add oxygen at the entrance of the hot probe which could enable the tar to be combusted. This would be an advantage as a purely aqueous solution is more simple to analyse using standard IC or ICP–OES laboratory equipment.

There was no former experience available on the extraction of the tar from the tubes and the filters. By personal inquiry to the laboratory of an oil refinery [30], a catalyst producing company [31], and a commercial laboratory [32], it was suggested to use an organic aromatic solvent combined with an alcohol. A solvent consisting of 90% toluene and 10% methanol was chosen as the components were available in analytical grade quality.

The tar material deposited in the alumina pipe and in the tubes was extracted using the chosen solvent. The filters were each placed in the solvent for ~30 min and extracted three times. This created 4 organic samples and three aqueous samples (based on solution A in Table 6) — a total of 7 subsamples for each of the ports L2–L4. At ports L5–L6 aqueous samples only were obtained based on solutions A and B, respectively.

The first row in Fig. 6 shows an overview of the samples as they arrived to the first laboratory. The three columns show samples L2A–L4A, L5A–L6A, and L5B–L6B respectively. The samples L2A–L4A were analysed at laboratory 1 (Lab. 1) for Na, K, and Ca for both the organic and the aqueous samples. 1 g of the organic samples was extracted during steady stirring to a sample glass and 5 mL analytical grade 68–70% HNO_3 was added to the sample glass. The sample was then treated for 90 min at 180 °C and 70 bar in a Perkin Elmer microwave oven to prepare the samples for analysis. After the treatment the liquid was transparent green with no solids and the gas phase was brown. The sample was then diluted with water to 25 mL and analysed on a Perkin Elmer, Optima 3000 DV Inductively Coupled argon Plasma torch with Optical coupled Spectrometer

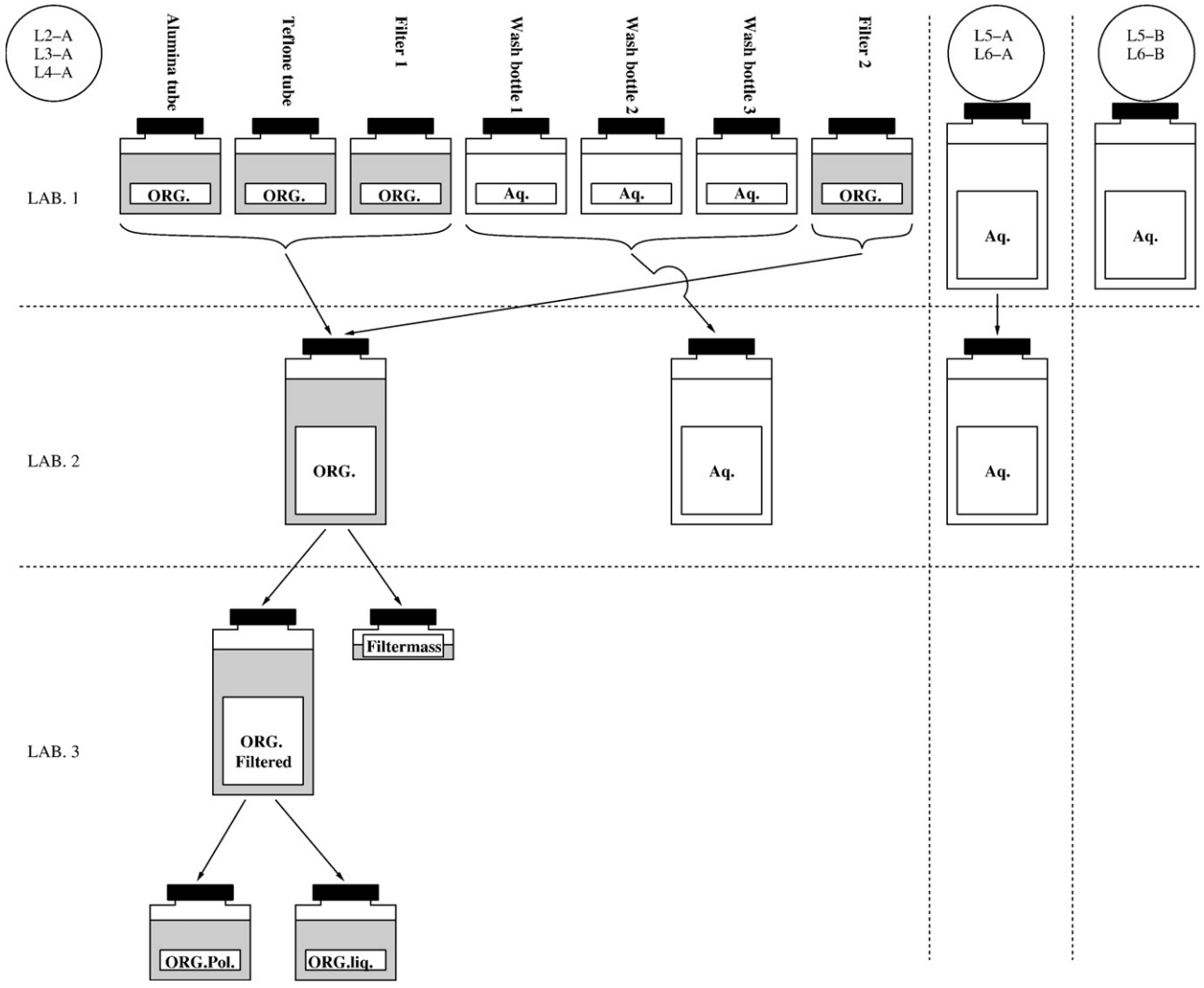

Fig. 6 – Overview of the history of the samples. The labels ORG. and Aq. denominate organic matter (diluted in 90% toluene and 10% methanol) and aqueous solution, respectively.

(ICP–OES). The aqueous samples of L2A–L4A and L5A, L6A, L5B, and L6B were not treated in microwave oven but otherwise followed the aforementioned procedure though for the L5B and L6B samples, standards for S, Pb, and Zn were used for the ICP analysis. Concentrations of Na, K, and Ca from ports L2–L6 were obtained. Concentrations of S, Pb, and Zn were obtained for ports L5 and L6.

The samples at this point were not analysed for Cl content since the first laboratory did not have capable equipment for measuring for Cl. The organic samples were collected in a single bottle for each of the L2A–L4A measurements and the same was done for the aqueous samples (see second row in Fig. 6). Laboratory 2 (Lab. 2) analysed the aqueous part of L2A–L4A for Cl and the samples L5A and L6A using Ion Chromatography (IC). The organic samples were treated with analytical grade 68–70% HNO_3 and subsequently diluted and analysed on IC together with a reference sample with known concentrations of NaCl and chloramphenicol. Only 20% of the organic chlorine in the reference sample could be found, thus the HNO_3 treatment followed by IC analysis was not suitable for preparing for Cl analysis.

The third laboratory (Lab. 3 — see third row in Fig. 6) had previous experience on cracking fuel-oil using H_2O_2 and water followed by 68–70% HNO_3 treatment. Lab. 3 had a recovery of 80% of an organic chlorine which is low, but reasonable compared to the previous 20% recovery. The organic samples of L2A–L4A were filtered using an analytical grade filter and toluene/methanol was added to retrieve all particles from the organic samples. The filtrated organic clear liquid was treated using H_2O_2 and water followed by HNO_3. The solution precipitated in what seemed to be a polymerised compound and some aqueous liquid. The aqueous liquid were analysed using Cl-capable ICP–OES but did not contain Cl in reliably measurable quantities (less than 1 mg/kg). The filtrated organic clear liquid was later analysed on an ICP–OES prepared for organic liquids, which is a less straightforward process compared to analysing aqueous solutions [33]. This analysis showed no measurable Cl-content (less than 2 mg/kg). The solids in the filter were treated with H_2O_2 and water followed by HNO_3 and analysed for Cl using ICP–OES. The Cl contribution from the organic samples originates solely from the solids captured in the filter.

All fractions were accounted for and it was therefore possible to use these procedures for analysis. However, the process was rather involved and complex, and a simplified method would be a significant improvement.

3. Results and discussion

Based on the video recordings, the visible combustion on the grate could be monitored. Combustion was highly irregular across the grate. Tongues of flames would sometimes stretch along part of the grate, while small islands of flames could exist further down the grate beyond the flame front as schematically represented in Fig. 7. Every 10th minute a frame from the video of the grate combustion was manually analysed by dividing each of the zones into smaller sub-zones. For example as shown in Fig. 7, zone L5 was divided into three parts across as $L5_r$, $L5_m$, and $L5_l$, and then the percentage of visible flame combustion was estimated for each of the sub-divided zones. No estimates of the percentage of flames on zone $L1_m$ were performed due to inability to see through the flames on the video. The values in $L5_m$ were based on a partly viewable grate (about 20%). An overview of the percentage of visible flames on the zones for three different days is shown in Fig. 8A–C. Fig. 8D shows average values of $L2_m$–$L5_m$ for each of Fig. 8A–C. Zones $L3_m$ and $L4_m$ are the zones which showed the greatest variance of the presence of a visible flame. $L2_m$ kept a level of 90–100% of flames coverage on average and $L5_m$ had below 10% flame coverage on average.

The personnel in the control room used the location and the extent of the visible flames to adjust the amount of primary air. If the visible flames reached beyond grate Section 3, additional primary air would manually be added especially to grate Sections 2–5, to ensure fully combustion of the waste before the final sections of the grate. Measured data for the average, standard deviation, minimum and maximum values of primary air obtained from Unit 5's surveillance and control system are shown in Fig. 9. The majority (61%) of the primary air was delivered to Sections 1–3. The standard deviation is greatest at Sections 2–5, which corresponds to the manual interference by the control room during operation. This resulted in the low average (5–28%) value of visible flames coverage on zone $L4_m$ as seen in Fig. 8D.

An overview of values of average, standard deviation, minimum and maximum temperatures measured by suction pyrometer for ports L2–L6 is shown in Fig. 10. The average temperature at port L3 was 1140 °C. This was considerably higher than the temperature at port L2 and port L4, which had average temperatures of 816 °C and 551 °C, respectively. At port L2, this could be explained by the drying of the waste still being an important factor. At port L4 the visible flames were

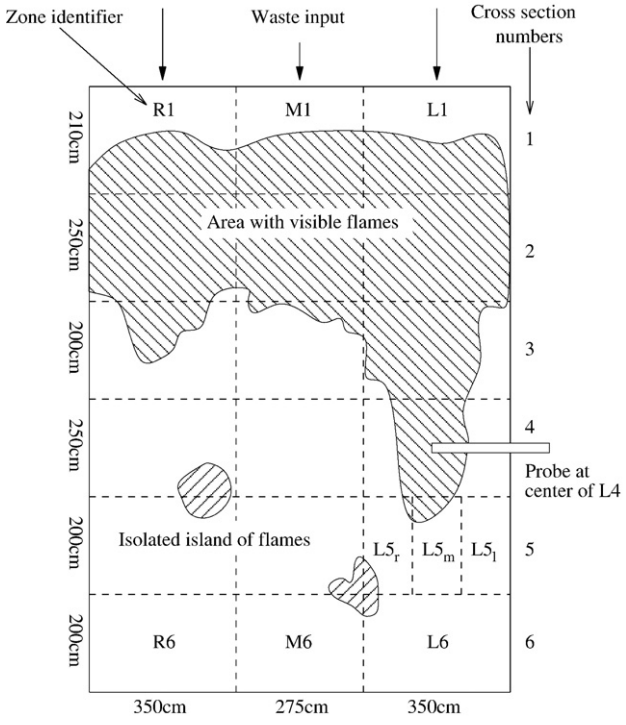

Fig. 7 – Highly irregular flamezones across grate.

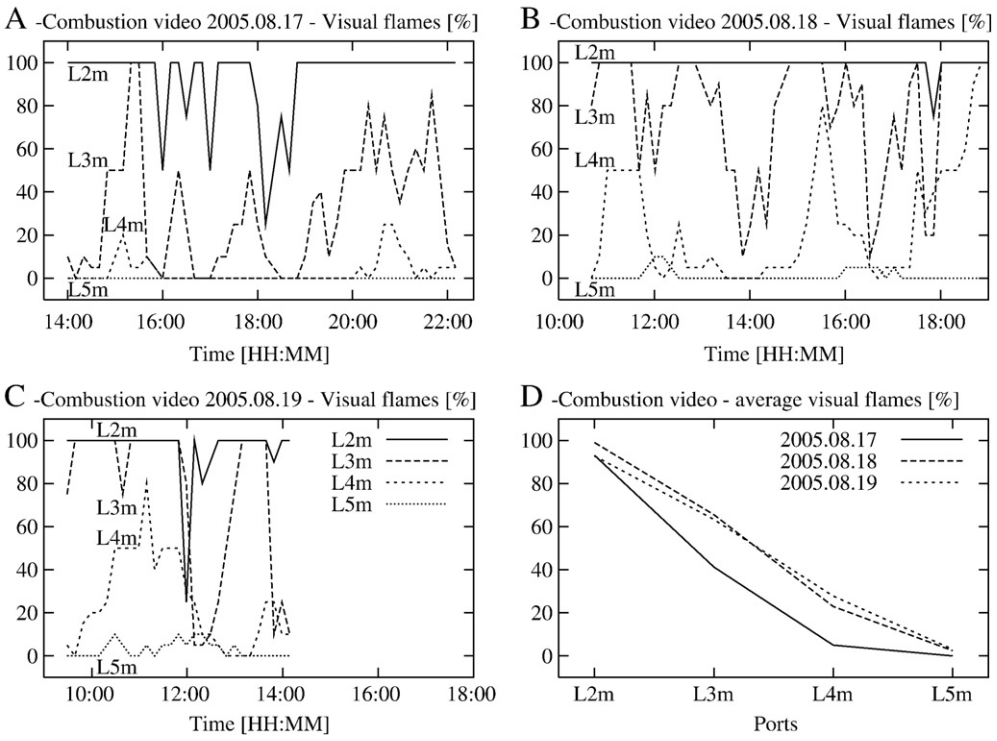

Fig. 8 – Overview of the amount of visible flames on the different grate zones L2m–L5m for three different days, and the average values for the zones of each sets of data.

rarely present, but the primary air was on average only 20% lower than the level of primary air at ports L2 and L3.

In Fig. 11 values of the gas concentration of O_2, CO and CO_2 are presented as function of the port location. The volume fraction of O_2 increased from zero at port L2 to 21% at port L6. The level of CO and CO_2 dropped from levels around 7% and 16% to averages of 0.18% and 0.04% at the end of the grate at port L6. The values of CO and CO_2 did not represent the total amount of carbon released from the grate as some of the carbon at ports 2 and 3, and port 4 were present as tar in the flue gas. The value of the O_2-concentration at port L5 is above 21%, which was too high compared to the oxygen concentration in atmospheric air. This was caused by excessive volumetric flue gas flow entering the gas analyser. At port L3 the standard deviation of O_2, CO and CO_2 was significantly higher than at any of the other ports. This compared well to the visible flames coverage in the same period as seen in Fig. 8A–C with the visible flames coverage from below 10% up to 100%. Fig. 12 shows the measured concentration-profiles of Cl, Na, K, and Ca along the left grate section. The concentration decreased for all the species along the grate, but at port L5 a sharp increase in concentration of Cl, K, and Na was seen. The high concentrations of Cl, K, and Na at port L5 are strange since the combustion seems to be completed. As seen on Fig. 11 little or no oxygen was consumed at port L5 and the average gas temperature was relatively low (528 °C±96 °C see Fig. 10). The secondary air above the grate zones was controlled manually and closed during the measurements, but the recirculation of the flue gas was left in automatic mode. This could explain the sudden concentration increase as flue gas from the first zones maybe transported downwards to zone L5.

There was no direct correlation between the amount of chlorine found and how much the corresponding zone was covered with visible flames. Visible flames cover an average of 50% of zone $L3_m$ (see Fig. 8D) and the average temperature was highest at this port. This suggested that chlorine was being volatilised in the early stages of the grate while the combustion continues with visible flames present and high temperatures. The measurements of the elemental concentrations in ports L2–L4, which were performed at the same time, showed a decrease of chlorine that was interpreted as chlorine being volatilised during

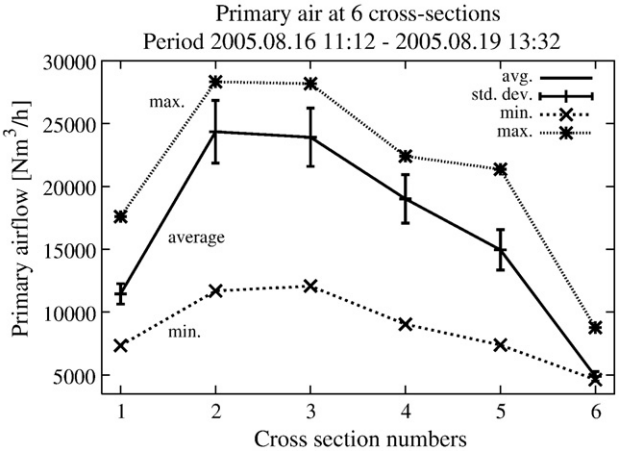

Fig. 9 – Average, standard deviation, minimum and maximum values of primary air in cross section (zones L+M+R) of the grate.

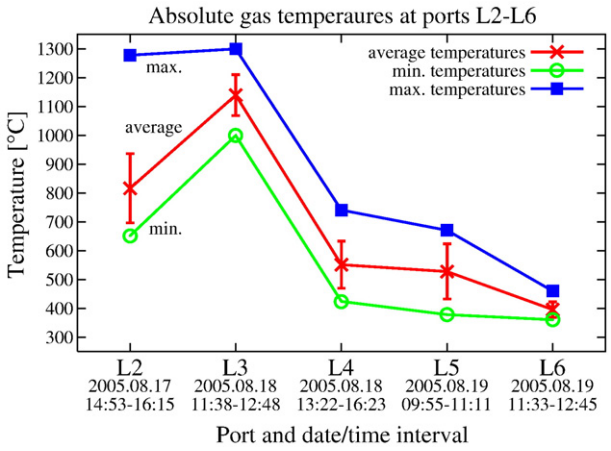

Fig. 10 – Temperature profile along the grate measured with suction pyrometer.

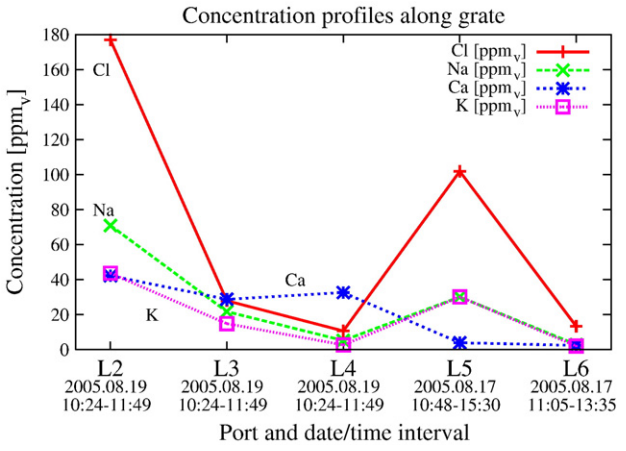

Fig. 12 – The concentration of species as function of location including the time when the sampling took place.

the early stages of the combustion. Table 7 shows the concentration of Pb, Zn, and S at the end of the grate at ports L5 and L6. The concentration of Pb and Zn was low and decreased from port L5 to L6. S had significantly higher level of concentration compared to any of the other elements at any of the other ports.

The results obtained for the concentrations are only supported by a single measurement at each of the ports. Thus it is not possible to confirm the reproducibility and the variance of the results over time for the measurement method.

Fig. 13 represents the relative percentage distribution of Na, K, and Ca through the sampling system. At ports L2–L4 more than 50% of Na, K, and Ca were found distributed in the alumina probe, Teflon tube, and the first filter. It would therefore be a large error not to include the contribution from the alumina tube, the Teflon tube, and the filter. The majority of Na and K in the aqueous solution is found in the first wash bottle and smaller fractions were found in wash bottles 2 and 3, which indicates 2 wash bottles to be sufficient for Na and K. At port L4 the concentrations of Na and K in are at the same low level indicating that very little reaches the wash-bottles. The concentration of Na and K decreases drastically from port L2 to L4 while the concentration of Ca only decreased slightly. Ca is primarily found in the alumina tube, in the Teflon tube, and in the filter (80–95%). The more steady release from L2 to L4 indicated the primary form of Ca to be particle-based.

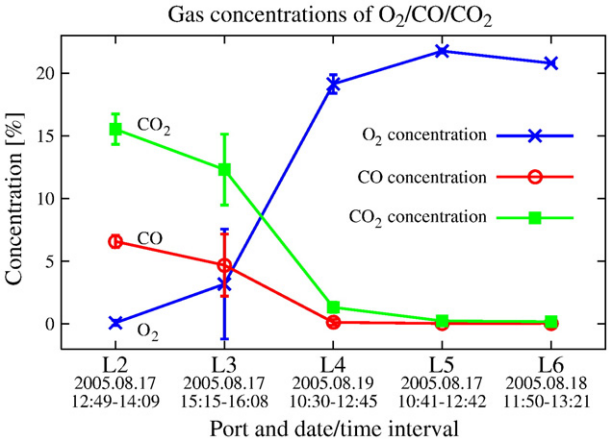

Fig. 11 – Overview of average values of O_2, CO and CO_2 along the grate.

4. Release and energy profile analysis

Fig. 14 shows the theoretical average flue gas concentration for different elements in the dry flue gas above the grate assuming the waste is using all possible primary air for the combustion. The theoretical average flue gas concentrations were estimated based on an average waste feed of $24{\cdot}10^3$ kg h^{-1}, a primary air flow of $97{\cdot}10^3$ Nm^3 h^{-1} and the mixed waste composition from Belevi [5] shown in Table 1. The fraction of the elements not released to the flue gas (remains in the bottomash — see Table 1) was also assumed. It was assumed that no water content was present in the primary air (compared to 1.63 mol/mol.% which would be present at 25 °C, at an estimated 50% relative humidity). The excess air ratio at these conditions was 0.86. The concentration levels are above those found by the measurements by approximately a factor 10. This can be explained partly by the missing measurements on port L1, and partly by the inherent variations in waste composition. Also incomplete dissolution of residues during the analytical preparations may lead to loss of some material. It is unlikely, however, to be able to fully explain the deviations seen between the theoretical and the measured values. The concentrations of Na and K in the flue gas prior to the flue gas clean-up have been estimated on the basis of the concentrations at ports L2–L4, the primary air at these ports, and the average flue gas flow reported from the surveillance system (134,000 Nm^{-3} h^{-1} ± 3000 Nm^{-3} h^{-1}). The latter was not given on a dry basis.

Table 7 – Concentration of Zn, Pb, and S the grate at ports L5 and L6

Port	Pb	Zn	S
	[ppm_v]	[ppm_v]	[ppm_v]
L5	0.0047	0.15	303
L6	0.0007	0.047	270

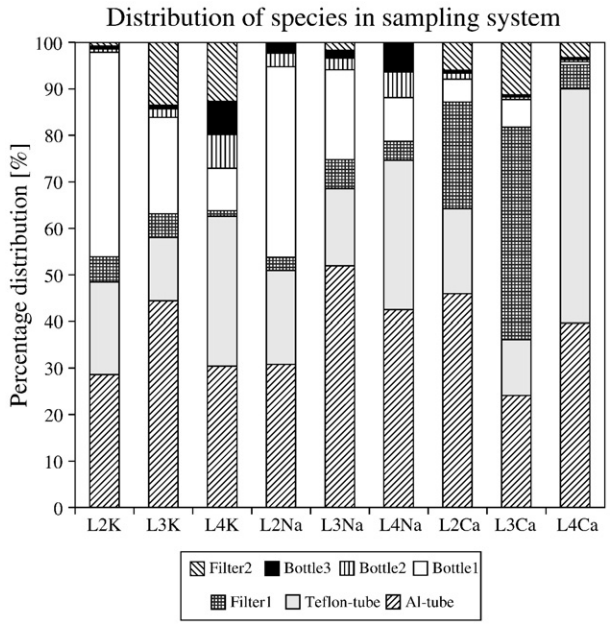

Fig. 13 – The distribution of elements Na, K, and Ca at port L2–L4 in percent.

Using the aforementioned assumptions and setting the release from sections L1, L5, and L6 to zero level, the concentrations of Na and K were calculated to be 17.5 ppm_v and 11.1 ppm_v, respectively. Poole et al. [15] reported concentrations of Na and K in the flue gas prior to gas clean-up in a grate fired waste incineration plant in the range 2–8 mg Nm^{-3} (2–8 ppm_v), and 4–8 mg Nm^{-3} (2–10 ppm_v), respectively. The differences in these values may be in the sampling-system where the Poole-system discarded the elements deposited in the sampling line, which is 40 m. However regional variations in waste composition and operating conditions may equally well influence these results.

In order to validate the results and to compare these to plant data, it was desired to review how much and where the heat was released from the grate sections.

Eqs. (1) and (2) are used to calculate the heat flux ($\dot{Q}$) delivered from each of the grate cross sections estimated as the enthalpy of the flue gas, $\hat{H}_{air}$, and the extra combustion

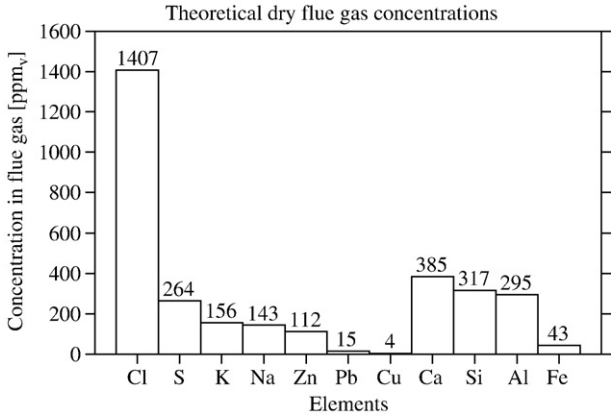

Fig. 14 – Theoretical flue gas concentrations.

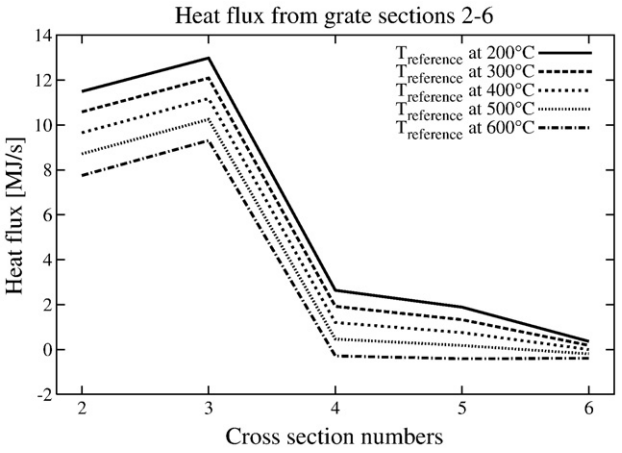

Fig. 15 – Heat split based MJ s^{-1}.

enthalpy provided by the CO reaction with O_2 (see Eq. (3)) in the flue gas (fg), $\hat{H}_{c,CO}(T_{fg})$. Combustion enthalpies from other organic species, such as tar, have not been taken into account for these equations. The enthalpy of the flue gas from the volatile species has not been taken into account, either.

$$\begin{aligned}\dot{Q} &= \dot{n}_{air}\hat{H}_{air} + \dot{n}_{CO}\hat{H}_{c,CO}(T_{fg}) \\ &= \dot{n}_{air}\int_{T_{fg}}^{T_{ref}} C_{p,air}dT \\ &\quad + \dot{n}_{CO}\left(\int_{T_{fg}}^{298K} C_{p,CO}dt + \frac{1}{2}\int_{T_{fg}}^{298K} C_{p,CO_2}dt + H^{\circ}_{fCO_2}(298K)\right)\end{aligned} \quad (1)$$

$$-H^{\circ}_{fCO}(298K) - \frac{1}{2}H^{\circ}_{f,O_2}(298K) + \int_{298K}^{T_{fg}} C_{p,CO_2}dt \quad (2)$$

$$CO + \frac{1}{2}O_2 \rightarrow CO_2 \quad (3)$$

C_p values are obtained using Eq. (4) with constants (a–d) from reference [34] assuming ideal gas and constant pressure.

$$C_p = a + bT + cT^2 + dT^3 \quad (4)$$

The heat flux from the flue gas is calculated as the heat released during cooling of the flue gas to a temperature (T_{fg}) in the range of 200–600 °C. The temperature span reflects a lower minimum super heater temperature and a maximum temperature above currently used super heater steam temperature in WtE plants (see Table 5).

The heat flux along the grate was estimated using Eq. (2) and shown in Fig. 15, which indicates the highest heat flux is emitted from Section 3.

The calculated heat flux from sections 2–6 is 29.4 MW based on the previous assumptions. This was well below the average heat output from electricity and heat of 14.4 MW and 55.16 MW delivered from the unit during the experiments. The heat produced from Section 1, the heat transferred to the waterwall and the heat content of the heavy volatiles may account for the differences between the calculated and the plant system values.

The majority of chlorine seems to be released at Section 2 (see Fig. 12) and Fig. 15 indicates the highest heat flux to occur at Section 3. Combining the heat release information with the

release of inorganic volatile species along the grate (Fig. 12) it seems that a high heat flux flue gas with a relatively low content of volatile species is provided from Section 3.

5. Conclusion

Measurements of gas concentrations (O_2, CO, and CO_2), element concentrations (Cl, Na, K, Ca, Pb, Zn, and S), and gas temperatures were conducted along the grate of a full-scale grate-fired waste incineration plant. The plant had 6 ports equally distributed along the grate and it was possible to measure at the last 5 of these ports. No measurements were performed through port L1 during the experiments due to the level of waste exceeding the port level. Video recordings documented the highly irregular behaviour of the flames of the waste being incinerated on the grate.

Accurate temperature data were obtained and a temperature profile was created with a temperature maximum of 1140 °C±71 °C at port L3.

The sampling system used for collecting the volatile species was not ideal for measurements in the early sections of the grate (L2–L4) due to tar that condensed in the tubes and filters.

Most of the elements Cl, Na, K and Ca were released at port L2 and a gradual decrease in concentration was observed at ports L3 and L4. The measured concentrations at port L2 was 177, 71, 44, and 42 ppm_v for Cl, Na, K, and Ca, respectively. However, at port L5 a relatively high concentration of Cl (102 ppm_v), Na (30 ppm_v), and K (30 ppm_v) was seen. This was thought to be influenced by the recirculation of flue gas moving some of the flue gas from sections L2–L4 to section L5.

6.6% and 4.7% CO were present at ports L2 and L3 respectively, with little or no O_2 present. The O_2 level increased to 21% at ports L5 and L6 however. The combustion took place primarily at grate Sections 2 and 3.

A heat flux profile from grate sections 2–6 was calculated from the combustion enthalpy of CO combined with the latent heat of the flue gas from those sections. There was an optimum in the heat flux from port L3 while at the same port the flue gas contained a relatively low content of the corrosive elements Cl (28 ppm_v), Na (22 ppm_v), and K (15 ppm_v).

Acknowledgements

The project was funded by the PSO Project 59281 and STVF (The Danish Technical Research Council) and performed by the CHEC research group at the Department of Chemical Engineering, Technical University of Denmark, and as part of the Nordic Graduate School of Biofuel Science and Technology. The authors would like to thank the technical staff at Vestforbrændning for their help during the tests.

REFERENCES

[1] P. Rademakers, W. Hesseling, J. van de Wetering, Review on corrosion in waste incinerators, and possible effect of bromine., Tech. rep., TNO Industrial Technology (2002).

[2] Y. Yang, V. Sharifi, J. Swithenbank, Effect of air flow rate and fuel moisture on the burning behaviours of biomass and simulated municipal solid wastes in packed beds, Fuel 83 (11-12) (2004) 1553–1562.

[3] A. Chandler, T. Eighmy, J. Hartlén, O. Hjelmar, D. Kosson, S. Sawell, H. van der Sloot, J. Vehlow, Municipal Solid Waste Incinerator Residues, Elsevier, 1997.

[4] H. Belevi, M. Langmeier, Factors determining the element behavior in municipal solid waste incinerators. 2. laboratory experiments, Environmental Science & Technology 34 (12) (2000) 2507–2512.

[5] H. Belevi, H. Moench, Factors determining the element behavior in municipal solid waste incinerators. 1. field studies, Environmental Science & Technology 34 (12) (2000) 2501–2506.

[6] H.H. Krause, Corrosion by chlorine in waste-fueled boilers, Incinerating Municipal and Industrial Waste: Fireside Problems and Prospects for Improvement, 1991, pp. 145–159.

[7] K. Nakagawa, Y. Matunga, Effect of HCl on the corrosion of waterwall tubes in a waste incineration plant, Science and Technology Letters (1997) 245–250.

[8] D. Albina, K. Millrath, N. Themelis, Effects of feed composition on boiler corrosion in waste-to-energy plants, 12th North American Waste To Energy Conference (NAWTEC 12), 2004.

[9] E. Latham, D.B. Meadowcroft, L. Pinder, The effedcts of coal chlorine on fireside corrosion, Incinerating Municipal and Industrial Waste: Fireside Problems and Prospects for Improvement, 1991, pp. 97–117.

[10] C.C. Chan, Behaviour of metals under the conditions of roasting msw incinerator fly ash with chlorinating agents, Journal of Hazardous Materials 64 (1) (1999) 75–89.

[11] C. Chan, C.Q. Jia, J.W. Graydon, D.W. Kirk, The behaviour of selected heavy metals in msw incineration electrostatic precipitator ash during roasting with chlorination agents, Journal of Hazardous Materials 50 (1) (1996) 1–13.

[12] L. Sørum, F. Frandsen, J. Hustad, On the fate of heavy metals in municipal solid waste combustion. Part II. from furnace to filter, Fuel 83 (11-12) (2004) 1703–1710.

[13] N. Watanabe, H. Ito, Analysis of waste for combustion: the case of osaka city, japan, Resources, Conservation and Recycling 20 (1997) 57–69.

[14] S.C. van Lith, Release of inorganic elements during wood-firing on a grate, PhD Thesis, Tecnical University of Denmark, Department of Chemical Engineering, CHEC Research Centre (2005).

[15] D.J. Poole, V. Nasserzadeh Sharifi, J. Swithenbank, D. Ardelt, Identification of metal concentration fluctuations in waste-to-energy plant flue gases-a novel application for ICP–OES, Journal of Analytical Atomic Spectrometry 20 (9) (2005) 932–938.

[16] E. Timmermans, F. de Groote, J. Jonkers, A. Gamero, A. Sola, J. van der Mullen, Atomic emission spectroscopy for the on-line monitoring of incineration processes, Spectrochimica Acta, Part B: Atomic Spectroscopy 58 (5) (2003) 823–836.

[17] H.-H. Frey, B. Peters, H. Hunsinger, J. Vehlow, Characterization of municipal solid waste combustion in a grate furnace, Waste Management 23 (8) (2003) 689–701.

[18] T. Jentsch, M. Beckmann, M. Davidovic, S. Biollaz, Investigation of heavy metal release during thermal waste treatment on a forward-acting grate by means of radiotracers, Chemical Engineering & Technology 26 (2003) 691–696.

[19] G. Sorrell, The role of chlorine in high temperature corrosion in waste-to-energy plants, Materials at high temperatures 14 (3) (1997) 207–220.

[20] M. Born, Cause and risk evaluation for high-temperature chlorine corrosion, VGB Powertech 5 (2005) 107–111.

[21] M. Spiegel, Corrosion science and technology — salt melt induced corrosion of metallic materials in waste incineration plants, Materials and Corrosion - Werkstoffe und Korrosion 50 (7) (1999) 373–393.

[22] R.W. Bryers, Fireside slagging, fouling, and high-temperature corrosion of heat-transfer surface due to impurities in steam-raising fuels, Progress in Energy and Combustion Science 22 (1) (1996) 29–120.
[23] G.J. Stanko, J.L. Blough, E.D. Montrone, P. Adkin, MSW corrosion: materials and design solution, Incinerating Municipal and Industrial Waste: Fireside Problems and Prospects for Improvement, 1991, pp. 261–278.
[24] H.P. Nielsen, F.J. Frandsen, K. Dam-Johansen, Lab-scale investigations of high-temperature corrosion phenomena in straw-fired boilers, Energy and Fuels 13 (6) (1999) 1114–1121.
[25] Babcock & Wilcox Vølund, Glostrup, Denmark, Director, Ole Hedegaard Madsen, Technology & Basic Engineering. URL http://www.volund.dk.
[26] Elsam Kraft A/S, Nordjyllandsværket, Denmark. Unit 3 has a capacity of 380 MW electricity and 420 MJ/s heat using a steam temperature of 582 °C and a steam pressure of 289 bar in 2004. URL http://www.elsam.dk.
[27] P. Henderson, C. Davis, M. Montgomery, A. Karlsson, In-situ fireside corrosion testing of superheater materials with coal, wood and straw fuels for conventional and advanced steam temperatures, VGB Powertech 85 (6) (2005) 53-59+6.
[28] A. Plumley, G. Kerber, W. Hermann, Gas-side corrosion and fouling in refuse-fired steam generators demonstrated by the würzburg CHP station, Incinerating Municipal and Industrial Waste: Fireside Problems and Prospects for Improvement, 1991, pp. 25–46.
[29] International Flame Research Foundation, IFRF. URL http://www.ifrf.org.
[30] Statoil A/S, Refinery at Kalundborg, Denmark, Laboratory Manager Claus Matschofsky. URL http://www.statoil.dk.
[31] Haldor Topsøe A/S, Nymøllevej 55, DK-2800 Lyngby, Denmark, Research and Development, Simon Ivar Andersen. URL http://www.topsoe.dk.
[32] SAYBOLT DENMARK A/S, Fyrtårnvej 11, DK-2300 København S, Danmark, Laboratory Manager Jan Akman. URL http://www.saybolt.dk.
[33] D. Weir, M. Blades, Characteristics of an inductively coupled argon plasma operating with organic aerosols part 1. spectral and spatial observations, Journal of Analytical Atomic Spectrometry 9 (12) (1994) 1311–1322.
[34] R.W.R. Richard, M. Felder, Elementary Principles of Chemical Processes, John Wiley & Sons, 1986.